EurJIC
European Journal of Inorganic Chemistry

Research Article
doi.org/10.1002/ejic.202500299

Chemistry Europe
European Chemical Societies Publishing

www.eurjic.org

Suppressing Spin–Phonon Relaxation and Enhancing Stability of Dysprosocenium Single-Ion Magnets via Metal-Organic Framework Confinement: A Theoretical Perspective

Garima Bangar[+], Reshma Jose[+], Rajanikanta Rana, and Gopalan Rajaraman*

Detailed ab initio CASSCF calculations coupled with periodic density functional theory studies on $[(Cp^*)Dy(Cp^{iPr5})]^+$ molecule encapsulated in a metal-organic framework (MOF) revealed that MOF encapsulation offers stability to these fragile molecules, keeping intact the U_{eff} (barrier height for magnetization reversal) values. Most importantly, this encapsulation suppresses the key vibrations responsible for reducing the blocking temperature, offering a hitherto unknown strategy for a new generation of SIM-based devices.

1. Introduction

Single-molecule magnets (SMMs) are a class of molecules that retain magnetization alike permanent magnets, below the blocking temperature (T_B).[1] They have garnered wide interest in the last decades due to their molecular-level information storage features, which offer potential applications in the fields of compact data storage, quantum computing, magnetic refrigeration, molecular spintronics, etc.[2] As very large T_B values are key to achieving the proposed compact data-storage application based on SMMs, there has been a concentrated effort over the last 10 years to improve the T_B value from liquid Helium to liquid nitrogen temperatures.[3] While this has been accomplished via a trial-and-error approach, the dysprosium-metallocene class of molecule is considered an important milestone as it raised the T_B significantly compared to other classes of compounds. Various chemical strategies have been evolved to improve the T_B above liquid-nitrogen temperatures using dysprosium single-ion magnets (SIMs) and this includes i) $[Dy(Cp^{ttt})_2]^+$ (Cp^{ttt}=1,2,4-tri(tertbutyl) cyclopentadiene) showing U_{eff} value of 1277 cm^{-1} and a T_B of 60 K,[4] ii) $[(Cp^{iPr4R})_2Dy]^+$ {R = Et, Me and Cp^{iPr4R} = 1,2,3,4-tetra(iso-propyl)-5-alkyl cyclopentadienyl} with U_{eff} value of 1380 cm^{-1} and a T_B of 66 K when R = Et and U_{eff} value of 1468 cm^{-1} and a T_B of 62 K when R = Me,[5] and iii) $[(Cp^*)Dy(Cp^{iPr5})]^+$ (Cp^{iPr5} = penta-iso-propylcyclopentadienyl, Cp^* = pentamethylcyclopentadienyl) with U_{eff} value of 1541 cm^{-1} and T_B = 80 K,[3b] exceeding the threshold of liquid nitrogen was synthesized, providing better linearity in the $Cp_{centroid}$–Dy–$Cp_{centroid}$ angles along with shorter Dy—C_{Cp} bonds. Enhancing the T_B value remains a key goal in this field. At the same time, realizing the proposed potential application requires molecules that are stable under ambient conditions—however, all the molecules (i)–(iii) are currently unstable. Several extensive experimental and theoretical studies suggest the role of enhancing the crystal field splitting, improving the linearity of $Cp_{centroid}$—Dy—$Cp_{centroid}$ angles and controlling molecular vibrations by shifting them to be in off-resonance with electronic excitation are shown to enhance the T_B values. Previously, theoretical predictions by our group demonstrated the potential of stabilizing reactive organometallic complexes inside nanoconfined spaces such as single-walled carbon nanotubes (SWCNTs), a prediction recently realized experimentally.[6] This success underscores the promise of encapsulation strategies for stabilizing highly reactive SMMs and inspired the present study. In this regard, we have explored the possibility of stabilizing this class of molecules inside a suitable metal-organic framework (MOF) using a combination of DFT and ab initio calculations (periodic DFT with PBE functional employing Cp2K suite[7] and complete active space self-consistent field (CASSCF)/RASSI-SO/SINGLE_ANISO using MOLCAS,[8] spin-vibronic relaxation was computed using the G09 suite;[9] see computational details). Our aim is to not only identify a suitable host material but also to investigate how encapsulation alters the electronic and vibrational properties of the molecule, with the goal of enhancing the blocking temperature. Encapsulation can lead to the quenching of spin–vibration coupling, a key factor limiting T_B. Lunghi and coworkers have recently highlighted the significant role of anharmonic phonons in driving under-barrier magnetization relaxation.[10] Therefore, spin–phonon coupling calculations are essential to uncover the fundamental mechanisms governing magnetic relaxation and to clarify how molecular motions influence this process. Such insights are vital for establishing design strategies that enable chemical tuning to suppress vibrational modes involved in Orbach and Raman relaxation pathways, ultimately guiding the development of high-performance SMMs. MOFs are an emerging class of porous materials built with

G. Bangar[+], R. Jose[+], R. Rana, G. Rajaraman
Department of Chemistry
Indian Institute of Technology Bombay
Powai, Mumbai, Maharashtra 400076, India
E-mail: rajaraman@chem.iitb.ac.in
[+]Both authors contributed equally.

Correction added on 29 August 2025, Correction regarding equal contribution of authors.

Supporting information for this article is available on the WWW under https://doi.org/10.1002/ejic.202500299

Research Article
doi.org/10.1002/ejic.202500299

the assembly of inorganic nodes and organic linkers to produce porous architectures.[11] The peculiar properties of MOFs, such as porosity, surface area, and chemical functionality, allow the tailoring of the MOF structure to complement the properties of the encapsulated unstable materials. There are several experimental precedents wherein SMMs, such as Mn_{12}, are stabilized inside a MOF, leading to better SMM characteristics.[12] Also, there are examples where unstable/non-isolable molecules are stabilized if a suitable MOF topology is offered.[13] Inspired by these studies, we have explored the possibility of stabilizing $[(Cp^*)Dy(Cp^{iPr5})]^+$ **(1)**[3b] in a suitable MOF. We selected MOFs over other porous materials because their tunable chemistry, permanent porosity, and crystalline nature provide an unmatched platform for systematic host–guest design and accurate structure–function correlations, critical factors for stabilizing and characterizing sensitive SMMs. Unlike COFs, which lack metal nodes, or ZIFs, which have limited pore chemistry and rigidity, MOFs excel in cation exchange, post-synthetic modification, and host–guest templating. These attributes make MOFs particularly well-suited for stabilizing delicate species like single-molecule magnets. Moreover, their exceptional crystalline structure enables detailed characterization using single-crystal X-ray diffraction, facilitating direct observation of host-guest interactions—a capability rarely achievable with COFs or ZIFs. Notably, while literature lacks studies on SMM encapsulation within ZIFs and COFs, MOF chemistry is firmly established in the realm of host–guest interactions.[14]An ideally suitable MOF should be i) diamagnetic, ii) the pore size should be suitable to enable stability, iii) MOF should be robust with permanent porosity and stable upon encapsulation, and iv) a suitable ligand framework, preferably aromatic linkers, so that **1** can be stabilized by non-covalent interactions.

To find the most suitable MOF, which fits the criteria (i)–(iv), we have used the QMOF Database,[15] as the QMOF database has 22,375 MOFs, we applied filters in the structural properties according to complex **1**. As the length of **1** is 7.6 Å. We gave a suitable range for pore-limiting diameter (6.5 to 8 Å) and largest cavity diameter (12.5 to 14.6 Å). The limiting value of 14.6 Å was given for the largest cavity diameter, considering a length of $[(Cp^*)Dy(Cp^{iPr5})]^+$ **(1)** plus additional space up to 3.5 Å each side for C−H•••π interactions. Applying this criterion yielded 65 candidate MOFs. To minimize magnetic interactions with the encapsulated Dy(III) complex, we prioritized the selection of a diamagnetic MOF. This has narrowed our search to eight suitable MOFs. We then modeled the encapsulation of complex **1** within these MOFs, and DFT calculations revealed favorable binding energies for two of them (see ESI Table S1, Supporting Information), with MOF-5 showing the most promising interaction. Thus, we narrow down the search to one experimentally synthesizable MOF, MOF-5 ($Zn_4O(BDC)_3$ (BDC = Benzene Di carboxylic acid) fulfilling all the criteria. The optimized geometries of **1** and MOF-5 are in agreement with the X-ray structure reported (Table S3, Supporting Information). Further ab initio CASSCF calculations were performed on **1** for both X-Ray and optimized structures using MOLCAS 8.2.,[16] which revealed magnetization relaxation via the fifth excited Kramer's doublet (KD) for both of them, yielding a barrier height of magnetization reversal (U_{cal}) value of 1390.9 and 1399.6 cm^{-1}, respectively (Figure S4, Supporting Information), showing close similarity. For our calculations, we have chosen a truncated model of MOF-5 (see Figure S2b, Supporting Information). To determine the most stable conformation of **1** inside MOF-5, we optimized different orientations or conformers of **1** inside MOF-5 (**Figure 1** and S5a, Supporting Information) ($\mathbf{1}^{edge}$@MOF, $\mathbf{1}^{face}$@MOF, and $\mathbf{1}^{vertex}$@MOF, where $\mathbf{1}^{edge}$@MOF is in which Cp ring is facing the edge of the cubic unit cell, i.e., linker moiety, $\mathbf{1}^{face}$@MOF is in which Cp ring is facing the face of the cubic unit cell, i.e., void space, and $\mathbf{1}^{vertex}$@MOF is in which Cp ring is facing the edge of the cubic unit cell, i.e., nodes of the MOF. The computed binding energy (BE) for $\mathbf{1}^{face}$@MOF (−215.6 kJ mol^{-1}) was higher compared to other orientations (see Table S5a, Supporting Information for BE details). Also, the Cp—Dy—Cp angle was comparatively slightly more linear (161.2^0) in $\mathbf{1}^{face}$@MOF, whereas a slight bending of the Cp—Dy—Cp angle was witnessed in $\mathbf{1}^{edge}$@MOF and $\mathbf{1}^{vertex}$@MOF. Further, to investigate the stability of various orientations, we have computed the possible C−H•••π interactions (in the range of 2.0−3.5 Å) in the system (Table S7, Supporting Information). There exist ≈19 strong C−H•••π interactions among C—H bonds of Cp^*/Cp^{ipr5} ring and π cloud of benzene linker of MOF-5 for $\mathbf{1}^{face}$@MOF, followed by 14 for $\mathbf{1}^{vertex}$@MOF and 11 for $\mathbf{1}^{edge}$@MOF, reaffirming the stability order of the orientations.

It is noteworthy that all models in this study are based on $[(Cp^*)Dy(Cp^{iPr5})]^+$@MOF-5, representing the encapsulation of cationic species. Magnetic anisotropy of Dy(III)-based SMMs is generally unaffected by the presence or absence of bulky counter anions, as these anions remain spatially distant from the Dy center and cause minimal electronic perturbation. However, due to the limited pore size of MOF-5, large counterions such as BPh_4^-, used in experimental studies,[3b] could not be incorporated into our model. To examine potential counterion effects, we performed geometry optimizations of **1**@MOF-5, including a smaller counteranion (BH_4^-) within the unit cell, allowing full structural relaxation. The system remained stable, with a negative binding energy, and the $\mathbf{1}^{face}$@MOF orientation retained the most favorable binding (–137.5 kJ mol^{-1}; see Table S5b, Supporting Information). However, due to its small size, BH_4^- is found to move closer toward the Dy center, reducing the $Cp_{centroid}$—Dy—$Cp_{centroid}$ angle and lowering magnetic anisotropy. While partial replacement of H by phenyl in the BH_4^- would prove effective, this has not been tested and suggests that counter anions also need to be screened side-by-side for optimal performance. Molecular migration studies of **1** (displaced by 3 Å) revealed multiple binding sites within the framework, with the center exhibiting the lowest repulsion and thus serving as the most favorable encapsulation site. The $\mathbf{1}^{face}$@MOF showed a highly anisotropic ground state ($M_J = \pm 15/2$) with negligible transverse components ($g_x = g_y = 0.0$ and $g_z = 19.978$) (Table S6, Supporting Information), where g_z axis passes through Dy by piercing the *Cp* rings. In the six lowest doublets, the crystal field (CF) exhibits a highly axial nature, with each state predominantly associated (greater than 96% character) with a definite projection of the total angular momentum, M_J (see Table S6,

Research Article
doi.org/10.1002/ejic.202500299

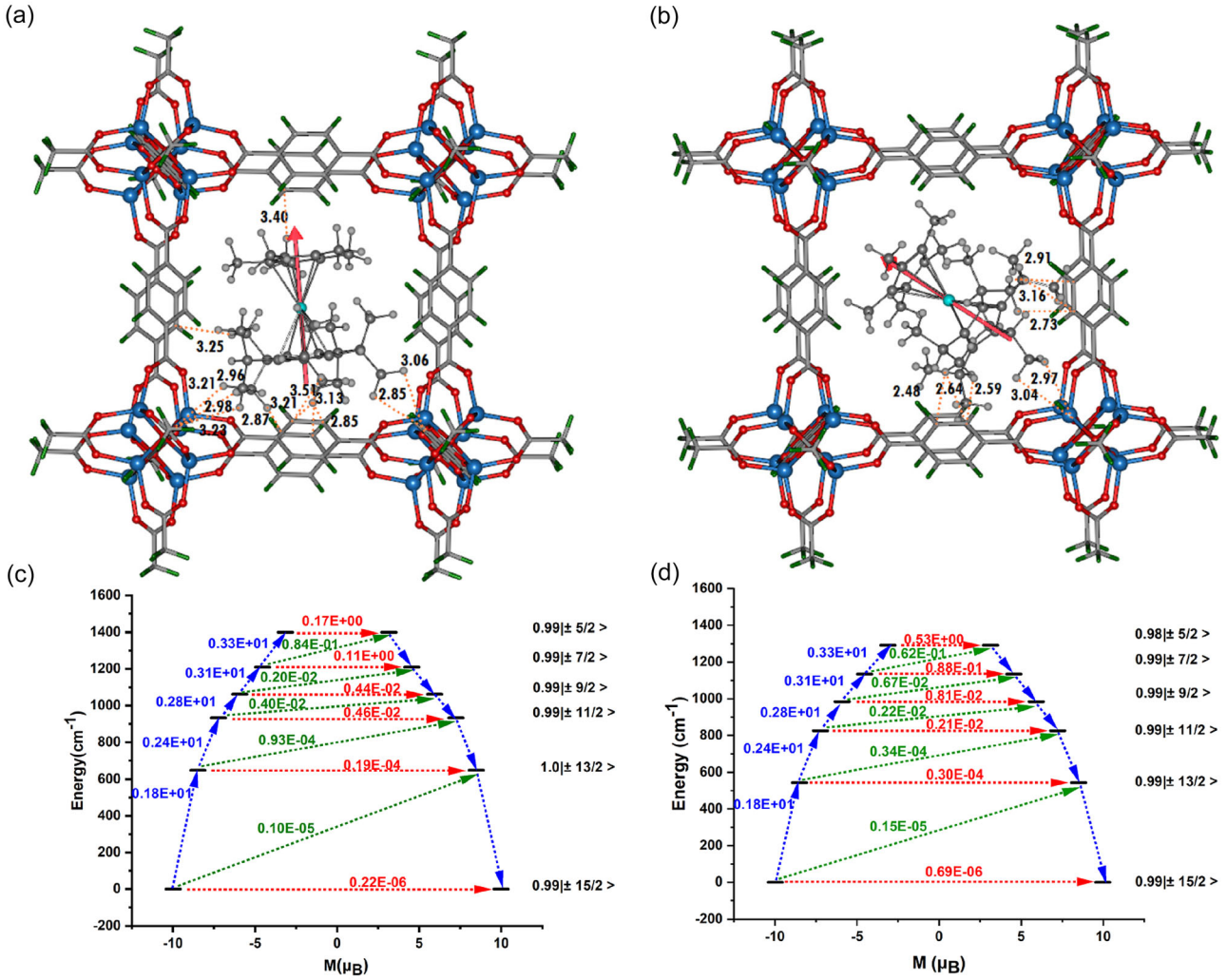

Figure 1. The DFT optimized structures: a) 1^{face}@MOF and b) 1^{vertex}@MOF. Dotted orange lines show C-H•••π. Color code: Dy(III)-cyan blue, C-gray, O-red, and Zn-blue. The red arrow shows the ground state g_z axis. c,d) Ab initio computed magnetization blockade barriers, along with computed transversal magnetic moments between the connecting pairs for complexes 1^{face}@MOF and 1^{vertex}@MOF, respectively.

Supporting Information). As the energy increases, the transverse components of the g-tensors roughly escalate by an order of magnitude in each doublet. Notably, up to the fifth doublet, the transverse components become non-negligible, and in the sixth doublet, they are substantial enough to permit significant tunneling. In the two highest states, axiality weakens, leading to considerable mixing under the influence of the crystal field, likely influenced by the asymmetry of the coordination environment. The U_{cal} value for $\mathbf{1}^{face}$@MOF is 1399.2 cm^{-1} (Figure 1c and S6, Supporting Information), while for **1**, the energy barrier for magnetization reversal is computed for Xray (optimized structure), where 1390.9 cm^{-1} (1399.6 cm^{-1}), and the magnetization relaxation occurs via the 5th excited state only. This suggests that the encapsulation of **1** inside MOF retains the U_{cal} value and simultaneously provides better stability to **1**.

Our study reveals the stabilization of the molecule upon encapsulation inside the MOF. Previous studies have shown that changes in barrier height do not consistently correlate with alterations in blocking temperature, a phenomenon attributed to spin-vibration coupling. To delve into this discrepancy, we conducted spin-vibration calculations. Employing a hybrid approach that combines density functional theory (DFT) with ab initio SA-CASSCF/RASSI-SO/SINGLE_ANISO methods, we investigated the electronic structure and spin-vibrational correlations of both the complex **1** and $\mathbf{1}^{face}$@MOF, aiming to elucidate their blocking temperatures comprehensively. Further details can be found in the Electronic Supporting Information (ESI).

To understand the role of the encapsulation of **1** inside MOF-5 in spin-vibration coupling, we have calculated the spin-vibrational coupling strength (S_j) for selected frequencies with significant oscillator strength behavior as depicted in **Figure 2** and Tables S9 and S10, Supporting Information. This analysis indicates that ω_{18} vibrational modes with strong coupling are probable contributors to magnetization relaxation. Additionally, the proximity of the first excited state of vibrational mode ω_{18} (524 cm^{-1} $((2+\frac{1}{2})\hbar\omega)$) compared to the KD1-KD2 (530 cm^{-1})

Research Article
doi.org/10.1002/ejic.202500299

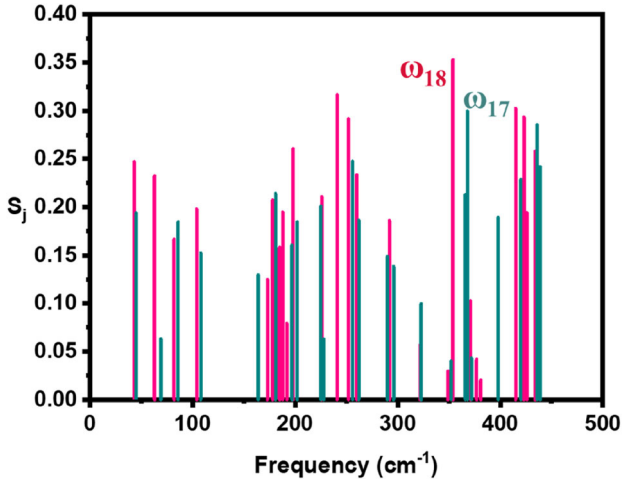

Figure 2. Ab initio calculated vibronic coupling strength (S_j) of the vibrational modes of **1** (red) and **1**^{face}**@MOF** (blue).

energy gap further supports its potential involvement in magnetization relaxation.

Further, we analyzed the S_j values for specific vibrational modes of **1**^{face}@MOF, as shown in Figure 2, Table S9 and S10, Supporting Information. This analysis reveals that vibrational modes with strong coupling, such as ω_{17}, are likely to influence magnetization relaxation. Additionally, the close proximity of the second excited state of the vibrational mode ω_{17} (540 cm^{-1}, $((2+\frac{1}{2})\hbar\omega)$) to the KD_1-KD_2 energy gap (537 cm^{-1}) further supports its significant role in magnetization relaxation. In both **1** and **1**^{face}@MOF, C—H vibrations are identified as contributing to relaxation, similar to what is commonly observed in $[(Cp^{ttt})_2Dy]^+$ type molecules (Figures S8, Supporting Information).

These calculations reveal a significant upward shift in vibrational modes when **1** is encapsulated inside the MOF. This shift indicates that the vibrational frequencies of the modes increase with the encapsulation of **1** inside MOF. Additionally, there is a noticeable decrease in the S_j value (Figure 2), which represents the vibronic coupling strength. This decrease suggests that the interaction between the spin states and vibrational modes weakens **1** encapsulated inside the MOF, offering a chance to enhance the T_B values by quenching the spin-vibronic relaxation mechanism via the Orbach process as well Raman process. Due to C—H…π interactions with the MOF framework, low-energy vibrational modes, particularly those involving out-of-plane C—H bending, shift to higher frequencies, as shown in the calculated IR spectra (Figure S9, Supporting Information). The high-spin vibronic mode shifts from 358 cm^{-1} (free molecule) to 368 cm^{-1} (encapsulated), indicating a stiffening of motion near π-systems. The IR intensity of this mode also decreases from 62.36 to 37.33 cm^{-1}, suggesting a reduced dipole moment change and redistribution of electron density. These out-of-plane bending and torsional modes are known contributors to magnetic relaxation; thus, their suppression via C—H…π interactions can enhance T_B.

To this end, we have proposed a way forward to solve multiple problems in achieving SIMs that can function at higher/room temperatures. The study unveiled how encapsulation within the MOF altered spin-vibronic coupling, suppressed QTM, induced frequency shifts, and enhanced molecular stability, shedding light on potential applications in magnetic materials research. Although our results predict favorable host–guest interactions and suggest a potential reduction in vibrationally driven relaxation pathways, this needs verification from experiments and this include other factors which are not fully explored and this includes but not limited to solubility mismatches, and the inherent fragility of both the dysprosocenium complex and the MOF-5 framework based on the MOF-5 synthesis method adopted.[17] However, prior work from our group reported the theoretical encapsulation of SMMs inside SWCNTs, predicting that C—H…π interactions, similar to this study, could stabilize the complex inside the SWCNT.[6] Notably, this theoretical prediction was subsequently verified experimentally by Yamashita and coworkers under high vacuum, while retaining its magnetic properties.[18]

Acknowledgements

We thank Science and Engineering Research Board (SERB) (CRG/2022/001697, SB/SJF/2019-20/12) for the funding.

Conflict of Interest

The authors declare no conflict of interest.

Data Availability Statement

The data that support the findings of this study are available in the supplementary material of this article.

Keywords: encapsulation · magnetism · metal-organic frameworks · single-molecular magnets

[1] R. Sessoli, D. Gatteschi, A. Caneschi, M. Novak, *Nature* **1993**, *365*, 141.
[2] L. Bogani, W. Wernsdorfer, *Nat. Mater.* **2008**, *7*, 179.
[3] a) F.-S. Guo, M. He, G.-Z. Huang, S. R. Giblin, D. Billington, F. W. Heinemann, M.-L. Tong, A. Mansikkamaki, R. A. Layfield, *Inorg. Chem.* **2022**, *61*, 6017; b) F.-S. Guo, B. M. Day, Y.-C. Chen, M.-L. Tong, A. Mansikkamäki, R. A. Layfield, *Science* **2018**, *362*, 1400.
[4] C. A. Goodwin, F. Ortu, D. Reta, N. F. Chilton, D. P. Mills, *Nature* **2017**, *548*, 439.
[5] K. R. McClain, C. A. Gould, K. Chakarawet, S. J. Teat, T. J. Groshens, J. R. Long, B. G. Harvey, *Chem. Sci.* **2018**, *9*, 8492.
[6] R. Nabi, R. K. Tiwari, G. Rajaraman, *Chem. Comm.* **2021**, *57*, 11350.
[7] T. D. Kühne, M. Iannuzzi, M. Del Ben, V. V. Rybkin, P. Seewald, F. Stein, T. Laino, R. Z. Khaliullin, O. Schütt, F. Schiffmann, *J. Chem. Phys.* **2020**, *152*, 194103.
[8] G. Karlström, R. Lindh, P.-Å. Malmqvist, B. O. Roos, U. Ryde, V. Veryazov, P.-O. Widmark, M. Cossi, B. Schimmelpfennig, P. Neogrady, *Comput. Mater. Sci.* **2003**, *28*, 222.
[9] R. A. Gaussian09, Inc., Wallingford CT **2009**, *121*, 150.
[10] a) A. Lunghi, F. Totti, S. Sanvito, R. Sessoli, *Chem. Sci.* **2017**, *8*, 6051; b) A. Lunghi, F. Totti, R. Sessoli, S. Sanvito, *Nat. Commun* **2017**, *8*, 14620; c) A. Lunghi, S. Sanvito, *J. Chem. Phys.* **2020**, *153*, 174113;

d) M. Briganti, F. Santanni, L. Tesi, F. Totti, R. Sessoli, A. Lunghi, *J. Am. Chem. Soc.* **2021**, *143*, 13633.
[11] a) H. Li, M. Eddaoudi, M. O'Keeffe, O. M. Yaghi, *Nature* **1999**, *402*, 276; b) H.C. Zhou, J. R. Long, O. M. Yaghi, *Introduction to Metal–Organic Frameworks*, vol. 12 ACS Publications, **2012**, *112*, 673.
[12] D. Aulakh, L. Liu, J. R. Varghese, H. Xie, T. Islamoglu, K. Duell, C.-W. Kung, C.-E. Hsiung, Y. Zhang, R. J. Drout, *J. Am. Chem. Soc.* **2019**, *141*, 2997.
[13] a) T. Zhang, K. Manna, W. Lin, *J. Am. Chem. Soc.* **2016**, *138*, 3241; b) F. Sha, Y. Chen, R. J. Drout, K. B. Idrees, X. Zhang, O. K. Farha, *iScience* **2021**, *24*, 102641; c) X. Xu, M. Ma, T. Sun, X. Zhao, L. Zhang, *Biosens.* **2023**, *13*, 435.
[14] a) X. Chen, R. Q. Xia, Q. M. Deng, Y. Q. Li, M. H. Chen, Y. G. Li, X. C. Cai, A. A. Titov, O. A. Filippov, E. S. Shubina, *Chin. J. Chem.* **2025**; b) D. Aulakh, L. Liu, J. R. Varghese, H. Xie, T. Islamoglu, K. Duell, C.-W. Kung, C.-E. Hsiung, Y. Zhang, R. J. Drout, *J. Am. Chem. Soc.* **2019**, *141*, 2997.
[15] A. S. Rosen, S. M. Iyer, D. Ray, Z. Yao, A. Aspuru-Guzik, L. Gagliardi, J. M. Notestein, R. Q. Snurr, *Matter* **2021**, *4*, 1578.
[16] F. Aquilante, J. Autschbach, R. K. Carlson, L. F. Chibotaru, M. G. Delcey, L. De Vico, I. Fdez, Galván, N. Ferré, L. M. Frutos, L. Gagliardi, *Molcas 8: New Capabilities for Multiconfigurational Quantum Chemical Calculations Across the Periodic Table*, Wiley Online Library, **2016**.
[17] J. Hafizovic, M. Bjørgen, U. Olsbye, P. D. Dietzel, S. Bordiga, C. Prestipino, C. Lamberti, K. P. Lillerud, *J. Am. Chem. Soc.* **2007**, *129*, 3612.
[18] H. Zhang, R. Nakanishi, T. Yoshida, M. Nishijima, K. Harano, Y. Horii, M. Yamashita, *Angew. Chem.* **2025**, *137*, e202503979.

Manuscript received: June 15, 2025
Revised manuscript received: July 30, 2025
Version of record online: August 23, 2025